Acta Oceanol. Sin., 2022, Vol. 41, No. 11, P. 58–72
https://doi.org/10.1007/s13131-021-1906-z
http://www.aosocean.com
E-mail: ocean2@hyxb.org.cn

Simulating the influence of various nutrient sources on hypoxia off the Changjiang River Estuary

Jingjing Zheng[1, 2, 3], Shan Gao[1, 2, 3*], Guimei Liu[1, 2], Yun Li[1, 2], Zhijie Li[1, 2], Xueming Zhu[1, 2, 3]

[1] National Marine Environmental Forecasting Center, Beijing 100081, China

[2] Key Laboratory of Research on Marine Hazards Forecasting, National Marine Environmental Forecasting Center, Beijing 100081, China

[3] Southern Marine Science and Engineering Guangdong Laboratory (Zhuhai), Zhuhai 519080, China

Received 31 July 2021; accepted 23 September 2021

Abstract

Hypoxia is increasingly reported off the Changjiang River Estuary with the confluence of multiple high volume nutrient sources. The Regional Ocean Modeling System coupled with a biological model was used to analyze the effect of different nutrient sources on the development of hypoxia off the Changjiang River Estuary. By comparing to observed data, our model suitably captured the regional dynamics of chlorophyll *a*, dissolved oxygen, and nutrient concentration. A series of sensitivity experiments were conducted to investigate the hypoxia response to the various nutrient sources, such as loading from the Changjiang River, Kuroshio and Taiwan Warm Current. Our model results indicated that nutrients from different sources significantly influenced the hypoxia off the Changjiang River Estuary, and it was mostly affected by nutrients sourced from the Kuroshio. The nutrients input from the Changjiang River had larger impacts on the hypoxia in the north of 30°N than that in the south of 30°N. The nutrients sourced from the Taiwan Strait had a least influence on the hypoxia off the Changjiang River Estuary.

Key words: hypoxia, nutrient, different source, Changjiang River Estuary

Citation: Zheng Jingjing, Gao Shan, Liu Guimei, Li Yun, Li Zhijie, Zhu Xueming. 2022. Simulating the influence of various nutrient sources on hypoxia off the Changjiang River Estuary. Acta Oceanologica Sinica, 41(11): 58–72, doi: 10.1007/s13131-021-1906-z

1 Introduction

Hypoxia is defined as dissolved oxygen (DO) concentrations less than 2 mg/L (Diaz and Rosenberg, 1995; Boesch and Rabalais, 1991). Hypoxic conditions threaten the life of marine aquatic organisms, especially benthic animals such as shrimp and crab (Karlson et al., 2002; Renaud, 1986). The occurrence of hypoxia in coastal bottom waters is an increasingly global phenomenon (Diaz and Rosenberg, 2008; Rabalais et al., 2010). Recently, the total volume of nutrients and other pollutants discharged into the Changjiang River has dramatically increased, which has greatly promoted primary production and thereby exacerbated hypoxia off the Changjiang River Estuary (Chen et al., 2017; Liu et al., 2015; Wang et al., 2021; Lu et al., 2017).

The formation and evolution of hypoxia off the Changjiang River Estuary are not only significantly related to the physical processes (wind, topography, tide), but also by the biogeochemical processes associated with nutrient loading from the Changjiang River, Taiwan Warm Current (TWC) and Kuroshio subsurface water (Li et al., 2011; Wang, 2009; Wei et al., 2007; Zhu et al., 2011; Zhou et al., 2010; Zhang et al., 2020; Große et al., 2020). It is generally accepted that the increased nutrient loads which promote primary production, increase the severity of hypoxia off the Changjiang River Estuary (Ning et al., 2011; Wang et al., 2015; Zhou et al., 2020).

The nutrient concentration off the Changjiang River Estuary can be attributed to the discharge of the Changjiang River, Kuroshio subsurface water, and Taiwan Warm Current. Based on two surveys in the winter and summer, Liu et al. (2000) reported that the Kuroshio subsurface water provided constant nutrient fluxes to the East China Sea (ECS) shelf, which were considerably greater than the Changjiang River inputs. Fang (2004) reported that the P fluxes discharged by the Changjiang River were relatively small compared to those from the Kuroshio and the Taiwan Strait. Chen (1996) confirmed that the nutrients in the ECS shelf were mainly sourced from the upwelling of Kuroshio subsurface water, particularly for phosphate. However, how the different sources of nutrients affect the hypoxia off the Changjiang River Estuary remains unclear. Moreover, among the numerous nutrients inputs from the Changjiang River, Kuroshio, and Taiwan Strait, which one is the dominant contributor to the hypoxia off the Changjiang River Estuary?

Primary production on the ECS shelf is commonly phosphate limited, especially in the Changjiang River plume where the water is rich in nitrite and silicate but relatively low in phosphate (Chen et al., 2004; Gong et al., 1996; Wang et al., 2015). Based on *in situ* observational data in 2003, Chen et al. (2006) reported that the mean ratios of N/P on the ECS shelf were 22.8±15.0 and 22.0±14.8 in June and August respectively, suggesting that the growth of phytoplankton was limited by phosphate, as the phytoplankton assimilate nitrogen (N) and phosphorus (P) with a Redfield ratio N:P=16:1. Recently, an N-based model was coupled with a three-dimensional hydrodynamic model to investigate the influence of river discharge, and wind on the extent of hypoxia off the Changjiang River Estuary (Zheng et al., 2016). However, this

Foundation item: The Fund of Southern Marine Science and Engineering Guangdong Laboratory under contract No. SML2020Sp008; the National Key Research and Development Program of China under contract Nos 2016YFC1401605 and 2016YFC1401802.
*Corresponding author, E-mail: gaos@nmefc.cn

model did not include P and therefore assumed that the growth of phytoplankton was only limited by light and nitrogen. In our study, we extend this ecological model to include dissolved inorganic P (DIP) to investigate the influence of different nutrient sources on the hypoxia off the Changjiang River Estuary.

2 Methods

2.1 *Field and satellite data*

ECS Environmental Monitoring Center had conducted interdisciplinary, comprehensive field surveys off the Changjiang River Estuary most years. In this study, cross-sectional survey denoted as blue dots in Fig. 1 was carried on August 20–25, 2011 and August 12–14, 2012, the sampling stations denoted as red dots in Fig. 1 were carried on August 10–25, 2011. Monthly average surface chlorophyll was extracted from MODIS data (http://oceancolor.gsfc.nasa.gov) inside the model domain and mapped onto the model grid.

2.2 *Physical model*

A 3-D hydrodynamic model based on Regional Ocean Modeling System (ROMS) was implemented in the ECS and validated against observation data (Zheng et al., 2016). This model was built for the ECS (22.3°–53.1°N, 114°–143°E) with a (1/15)° horizontal resolution (Fig. 1a). The model contains 30 vertical layers, with increased resolution near the surface and bottom.

The model was initialized with climatological temperature and salinity from the Generalized Digital Environment Model (GDEM) (Carnes, 2009). The climatological data of Simple Ocean Data Assimilation (SODA, http://dsrs.atmos.umd.edu/DATA/soda_2.2.4/) provided the temperature, salinity, and sea level measurements at open boundaries. Atmospheric forcing was derived from National Centers for Environmental Prediction/Climate Forecast System Reanalysis (NCEP/CFSR) reanalysis products (http://rda.ucar.edu/datasets/ds093.0), including 6 hourly wind stress, net heat flux, freshwater flux, and shortwave radiation. The tidal forcing at open boundary consists of 10 constituents (M_2, S_2, N_2, K_2, K_1, O_1, P_1, Q_1, Mf, Mm) are extracted from the global inverse tide model TPXO7.2 of Oregon State University (Egbert and Erofeeva, 2002). The freshwater discharge of the Changjiang River was implemented from monthly mean observations of the Datong Hydrologic Station (Gao et al., 2012).

2.3 *Biological model*

The hydrodynamic model was coupled with a nitrogen cycle model previously published by Fennel et al. (2006). This model included 10 state concentration variables: nitrate (NO_3^-), ammonium (NH_4^+), phytoplankton (Phy), zooplankton (Zoo), chlorophyll (Chl), Small detritus (SDet), Large detritus (LDet), oxygen (Oxyg), total inorganic carbon (TIC), and total alkalinity (TALK). In the model, the sources of DO were air–sea gas exchange and primary production, and the sink included the zooplankton excretion, nitrification, detritus remineralization and sediment oxygen consumption (Fennel et al., 2013).

For this study, the model was extended to include DIP. DIP is absorbed by phytoplankton and released through the excretion by zooplankton, remineralization of detritus in the water column and sediment. Phytoplankton growth is limited by temperature, light and nutrients. It was assumed that the uptake of DIP in the model by phytoplankton follows Michaelis-Menten dynamics, with nutrient limitation mainly determined by the most limiting nutrient, DIN (N limitation, includes NO_3^- and NH_4^+) or DIP (P limitation). In the model we used the limitation factors $L_N = L_{NO_3^-} + L_{NH_4^+}$ for N and L_P for P. They were calculated as follows:

$$L_{NO_3^-} = \frac{[NO_3^-]}{k_{NO_3^-} + [NO_3^-]} \cdot \frac{1}{1 + [NH_4^+]/k_{NH_4^+}}, \quad (1)$$

$$L_{NH_4^+} = \frac{[NH_4^+]}{k_{NH_4^+} + [NH_4^+]}, \quad (2)$$

$$L_N = L_{NO_3^-} + L_{NH_4^+}, \quad (3)$$

$$L_P = \frac{[DIP]}{k_{DIP} + [DIP]}, \quad (4)$$

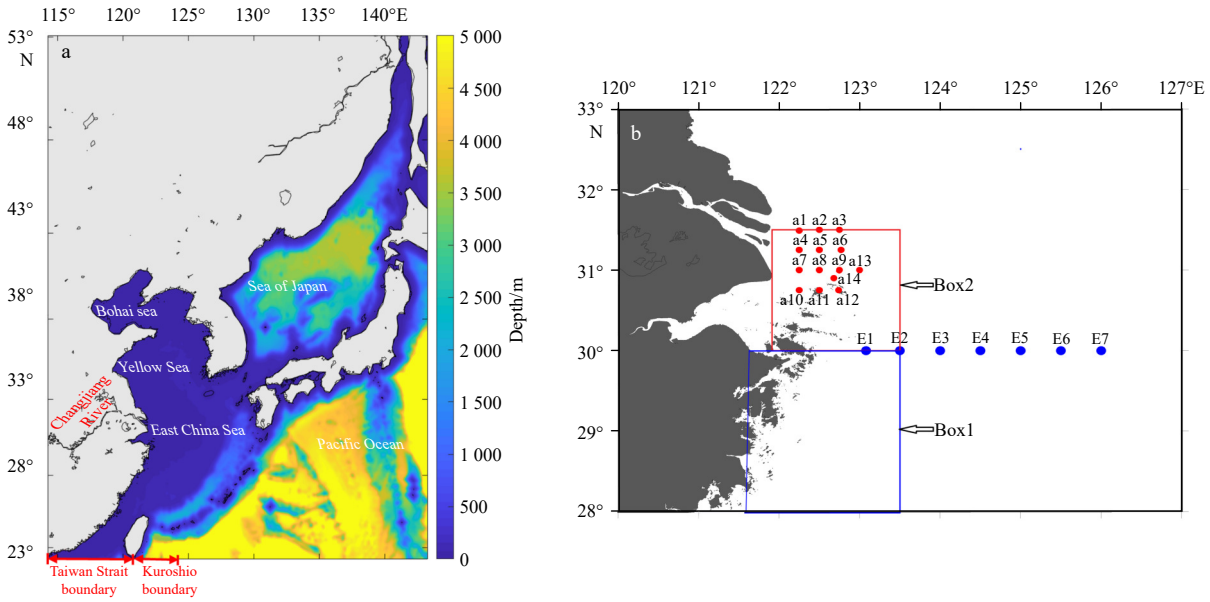

Fig. 1. Model domain and water depth (a), the red two-way arrows indicate the Taiwan Strait boundary and Kuroshio boundary, respectively. In b, Red dots represent station observation in August 2011; blue dots represent observations in August 2011, 2012. The blue and red rectangles indicate Box1 and Box2, respectively.

where [] means concentrations of components; the $k_{NO_3^-}$, $k_{NH_4^+}$ and k_{DIP} were the half-saturation for the NO_3^-, NH_4^+ and DIP uptake by phytoplankton, respectively. The values of $k_{NO_3^-}$, $k_{NH_4^+}$ and k_{DIP} were set to 0.5 mmol/m^3 (in terms of N), 0.5 mmol/m^3 (in terms of N) and 0.03 mmol/m^3 (in terms of P). The list of biological parameters is presented in Table 1.

The growth rate of phytoplankton was closely related to the light, temperature, and nutrient limitation. It was calculated as

$$u = u_{\max}(T) \cdot f(E) \cdot \min(L_N, L_P), \quad (5)$$

where $u_{\max}(T)$ was the maximum growth rate of phytoplankton, which was limited by temperature, and $f(E)$ was the function of photosynthesis-irradiance relationship.

At the sediment-water interface, the model assumed "instantaneous remineralization" by the organic matter (Fennel et al., 2006, 2013). This represents organic matter that is instantaneous remineralized into NH_4^+ and PO_4^{3-} when reaching the sediment. All P returned to the water column as PO_4^{3-}, but a constant fraction of N is lost through denitrification in the sediment.

The initial and boundary conditions for NH_4^+, PO_4^{3-}, DO derived from the World Ocean Atlas 2009 (WOA2009, http://www.nodc.noaa.gov/OC5/WOA09/pr_woa09.html). The initial and boundary values of ammonium were set to homogeneous, value of 1 mmol/m^3. The initial field of Chl was provided by SeaWiFS monthly climatological data. SeaWiFS has only surface data, so the initial value of Chl in the vertical direction was based on the formula proposed by Morel and Berthon (1989). The initial and boundary values of phytoplankton, zooplankton, and detritus concentrations were set to 0.5, 0.25, and 0.25 times the Chl concentration, respectively (Liu et al., 2002). The nutrients of the Changjiang River from the four seasonal surveys were based on previously reported data (Chen et al., 2012; Gao et al., 2012; Wang et al., 2016).

The physical model was spun up for 10 years driven by climatological forcing, and then the coupled physical-biological model was run from January 1, 2006 to December 31, 2012 by realistic forcing. A series of numerical experiments in 2010 were set up to study the influence of different nutrient sources (the Changjiang River, Taiwan Strait, and Kuroshio intrusion) on the hypoxia off the Changjiang River Estuary.

2.4 *Sensitivity experiments*

Excess nutrient loading from the Changjiang River enhances primary production and promotes the expansion of hypoxia off the Changjiang River Estuary. However, numerous studies suggested that the nutrients from the Taiwan Strait and Kuroshio were the major sources in the ECS (Chen and Wang, 1999; Li et al., 2014; Zhang et al., 2007). In order to study the effect of nutrients from the Changjiang River, Taiwan Strait and Kuroshio on the hypoxia off the Changjiang River Estuary, four sensitivity experiments were conducted. Case1 set the nutrients from sea surface to the bottom along the southern boundary (from 114°E to Taiwan Island) to 0 mmol/m^3, which considered only the nutrients from the Changjiang River and Kuroshio. In Case2, the concentration of nutrients from the sea surface to the bottom along the southern boundary (from the Taiwan Island to 124°E) where Kuroshio water occupied was set to 0 mmol/m^3, which considered the nutrients from the Changjiang River and Taiwan

Table 1. The parameters used in ecosystem model

Parameter	Value	Unit
Light attenuation by chlorophyll	0.024 86	m^{-1}
Light attenuation due to seawater	0.04	$(mg{\cdot}m^2)^{-1}$ (in terms of chlorophyll)
half-saturation for phytoplankton NO_3^- uptake	0.5	mmol/m^3 (in terms of N)
half-saturation for phytoplankton NH_4^+ uptake	0.5	mmol/m^3 (in terms of N)
half-saturation for phytoplankton PO_4^{3-} uptake	0.03	mmol/m^3 (in terms of P)
Phytoplankton, initial slope of P-I curve	0.025	mol/(g·W·m^2·d) (in terms of C)
Phytoplankton growth rate	0.69	d^{-1}
Zooplankton maximum growth rate	0.6	m^3/(mmol·d) (in terms of N)
Zooplankton half-saturation constant for ingestion	2	(mmol/m^3)^2 (in terms of N)
Phytoplankton mortality rate	0.15	d^{-1}
Maximum chlorophyll to carbon ratio	0.053 5	mg chlorophyll per mg C
Nitrification rate: oxidation of NH_4^+ to NO_3^-	0.05	d^{-1}
Half-saturation radiation for nitrification inhibition	0.1	W/m^2
Radiation threshold for nitrification inhibition	0.009 5	W/m^2
Zooplankton nitrogen assimilation efficiency	0.75	–
Zooplankton mortality rate	0.025	d^{-1}
Zooplankton basal metabolism	0.1	d^{-1}
Zooplankton specific excretion rate	0.1	d^{-1}
Large detritus remineralization rate N-fraction	0.1	d^{-1}
Small detritus remineralization rate N-fraction	0.2	d^{-1}
Large detritus remineralization rate C-fraction	0.1	d^{-1}
Small detritus remineralization rate C-fraction	0.2	d^{-1}
Coagulation rate	0.05	d^{-1}
Vertical sinking velocity for phytoplankton	0.5	m/d
Vertical sinking velocity for large detritus	5.0	m/d
Vertical sinking velocity for small detritus	2.0	m/d

Note: – represents no dimension.

Strait (Fig. 1b). Case3 set the nutrients input from the Taiwan Strait and Kuroshio to 0 mmol/m^3, which considered only the nutrients from the Changjiang River. To investigate the impacts of nutrients input from the Changjiang River on the hypoxia off the Changjiang River Estuary, the Case4 set riverine nutrients to zero. In the Base run, the nutrients input from the Changjiang River, Taiwan Strait, Kuroshio were all included (Table 2).

3 Results

3.1 *Model verification*

The spatial distribution of the modeled surface Chl was in agreement with satellite observations (MODIS) in September 2010 in Fig. 2. The root mean square error (RMSE) of surface Chl was 1.31 mg/m^3. In the Box1 and Box2 (Fig. 1b), the modeled results compared well with the satellite observations, showing high surface Chl adjacent to the Changjiang River plume and the Zhejiang coast. Surprisingly, another high value of modeled surface Chl was found in the areas of 30°–31.5°N, 124°–126°E. This will be explained in the Section 4.3.

Table 2. Model sensitivity experiment

	Nutrients input source
Base	Changjiang River +Taiwan Strait + Kuroshio
Case1	Changjiang River + Kuroshio
Case2	Changjiang River + Taiwan Strait
Case3	Changjiang River
Case4	Kuroshio + Taiwan Strait

Both the model and observational data captured the high PO_4^{3-} concentration (>0.5 mmol/m^3) at the bottom, but low (<0.2 mmol/m^3) at the surface along the section at 30°N in August 2011 (Fig. 3). The PO_4^{3-} contours near the coast tilt downward, which suggests the existence of the upwelling.

DO simulated results were consistent with observed data, showing high DO concentration in surface layer and low DO concentration in bottom layer along the section at 30°N in August 2011 and 2012 (Fig. 4). In August 2011, both simulated and observed bottom minimum DO concentrations were less than 4 mg/L. The modeled maximum DO concentration in the surface layer was 7 mg/L, and the observed maximum DO concentration was 8 mg/L. In August 2012, the hypoxic zone with DO less than 3 mg/L was captured by the model and observation along the section at 30°N. The maximum value of DO in the surface layer of the model and observation was 7 mg/L.

Figure 5 illustrates the comparison between the *in situ* and model results of NO_3^-, PO_4^{3-} and DO concentrations at the stations in August 2011 (Fig. 1b). The RMSE of surface NO_3^-, PO_4^{3-} and DO concentrations were 1.61 mmol/m^3, 0.173 mmol/m^3, 0.66 mg/L, respectively. The mean bias (MB) is defined as the difference between average value of model and observation. The MB of surface NO_3^- concentration between the model and observation was acceptable (–0.47 mmol/m^3). With regard to the surface PO_4^{3-} concentration, MB is 0.012 mmol/m^3, which indicates that the model overestimated the surface PO_4^{3-} concentration on average. The surface DO concentration performed significantly

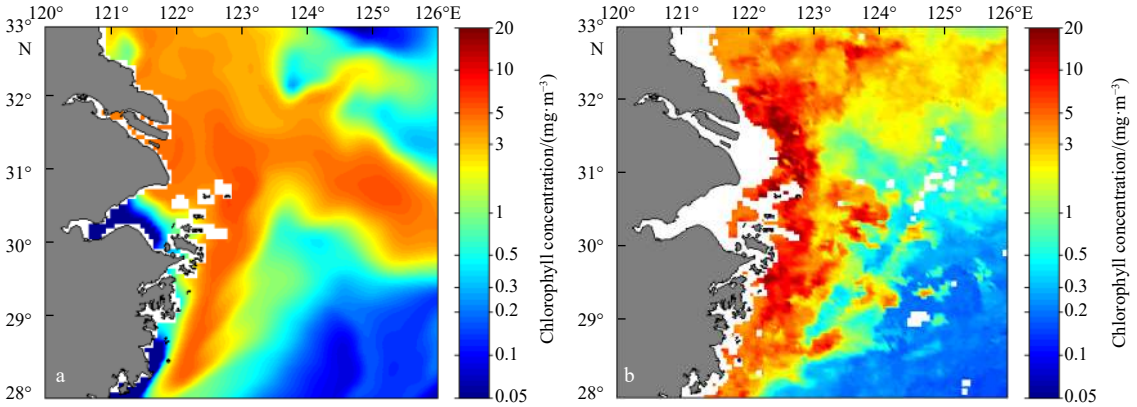

Fig. 2. Monthly averaged sea surface chlorophyll concentration from the model (a) and MODIS data (b) in September 2010.

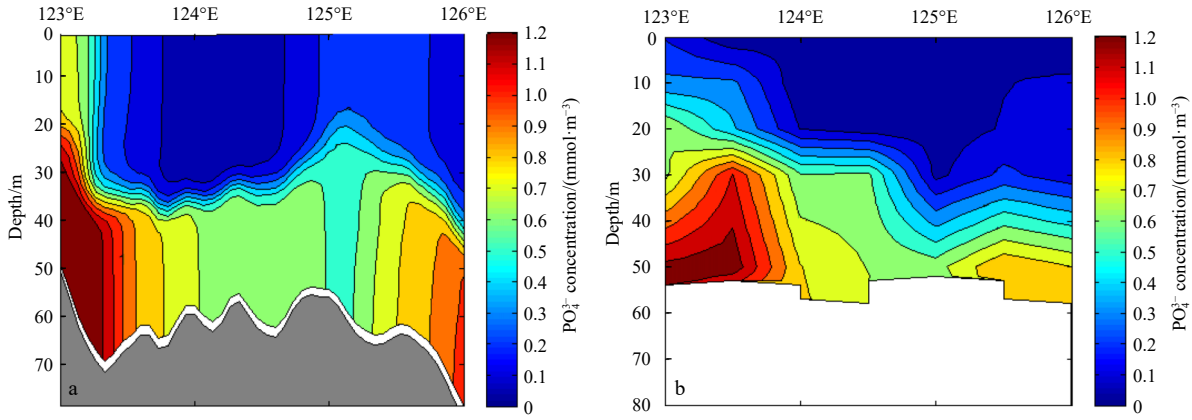

Fig. 3. The PO_4^{3-} concentration distribution along the section at 30°N in August 2011 from the model (a) and observation (b).

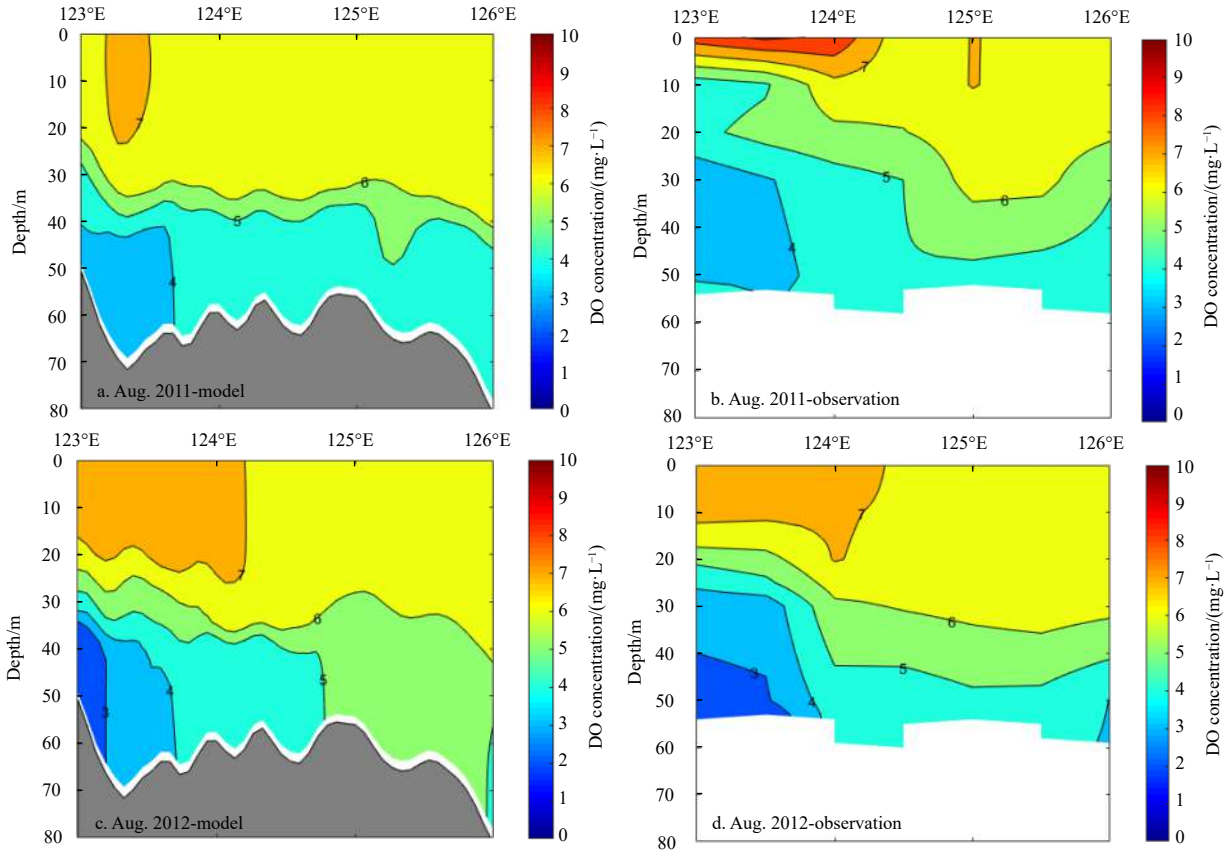

Fig. 4. The distribution of DO concentration along the section at 30°N in August 2011 (a, b) and 2012 (c, d) from the model (a, c) and observation (b, d).

better with MB=0.06 mg/L. The concentration of DO in the surface layer is generally high (>6 mg/L).

In Fig. 6, the model results reveal that it can capture the pattern of the circulation in the ECS, such as the Kuroshio, TWC and Changjiang diluted water (CDW). There were strong northeast streams originating from the Taiwan Strait (Fig. 6a). It flowed mostly parallel to the coastline until 28.5°N, and then divided into two branches. The offshore branch flowed east and then northwest before heading into the Tsushima Strait. The inshore branch was so weak that it was not easily distinguished from the surface circulation. It extended northward to the Changjiang River Estuary along the Zhejiang coast. The distribution of TWC in the model was comparable to *in situ* observations (Hu et al., 2010; Isobe, 2008). The strong Kuroshio originated from east of the Taiwan Island and flowed northeast into the ECS. The CDW flowed southwestward along the Zhejiang coast and became a major part of the Zhejiang coastal current. At the bottom, a branch of the Kuroshio Current flowed northwest from the northeast of Taiwan Island, and then flowed northeastward affected by the terrain after reaching 28°N. In the process of northward intrusion, the Kuroshio gradually weakened and was divided into two branches near 29°N. One branch was weak and continued to intrude northward until 31°N, while the second flowed northeast into the Tsushima Strait along the continental slope.

3.2 *Hypoxia variability off the Changjiang River Estuary*

Hypoxia is generally defined as DO concentration <2 mg/L (Diaz and Rosenberg, 1995), although in some studies it has also been defined as DO concentration <3 mg/L (Chen et al., 2007; Zhou et al., 2017). In our study, hypoxia is denoted as DO concentration <2 mg/L, and we use the term "Low DO" for DO concentration between 2 mg/L and 3 mg/L. There was significant variability of hypoxia in the ECS in July to October (Fig. 7). In July, no hypoxia was present and only two zones (south, north corner) indicated Low DO conditions (Fig. 7a). The southern zone of Low DO was larger than the north, and extended northeastward along the isobaths from the southwestern and reached as far as nearly 30.5°N. In general, DO concentration was lower in the south part of the study area, with the minimum DO concentration reaching 2.1 mg/L, which was close to hypoxia. In August, the DO concentration in the bottom was significantly decreased, and the minimum DO concentration was less than 2.0 mg/L. Hypoxia occurred off the Changjiang River Estuary in a small area in the north of 31°N. In September, the hypoxic zone off the Changjiang River Estuary further expanded. There were two zones where DO concentration was less than 2 mg/L and the minimum DO concentration was less than 1 mg/L. In October, the DO concentration in the bottom water off the Changjiang River Estuary significantly increased, and the hypoxic zone was disappeared. The bottom water DO concentration in the northern part was mostly greater than 3.0 mg/L, but remained low in the south (<3.0 mg/L). This model captured the seasonal variation of hypoxia, and the simulated results of DO concentration resembled the observed data (Wang et al., 2012).

3.3 *Hypoxia response of P limitation*

In order to investigate the influence of P limitation on the hypoxia, two types of simulation were conducted. The first was the control simulations (Base), which used the complete model with DIP. The second (N-only simulations) included only the ori-

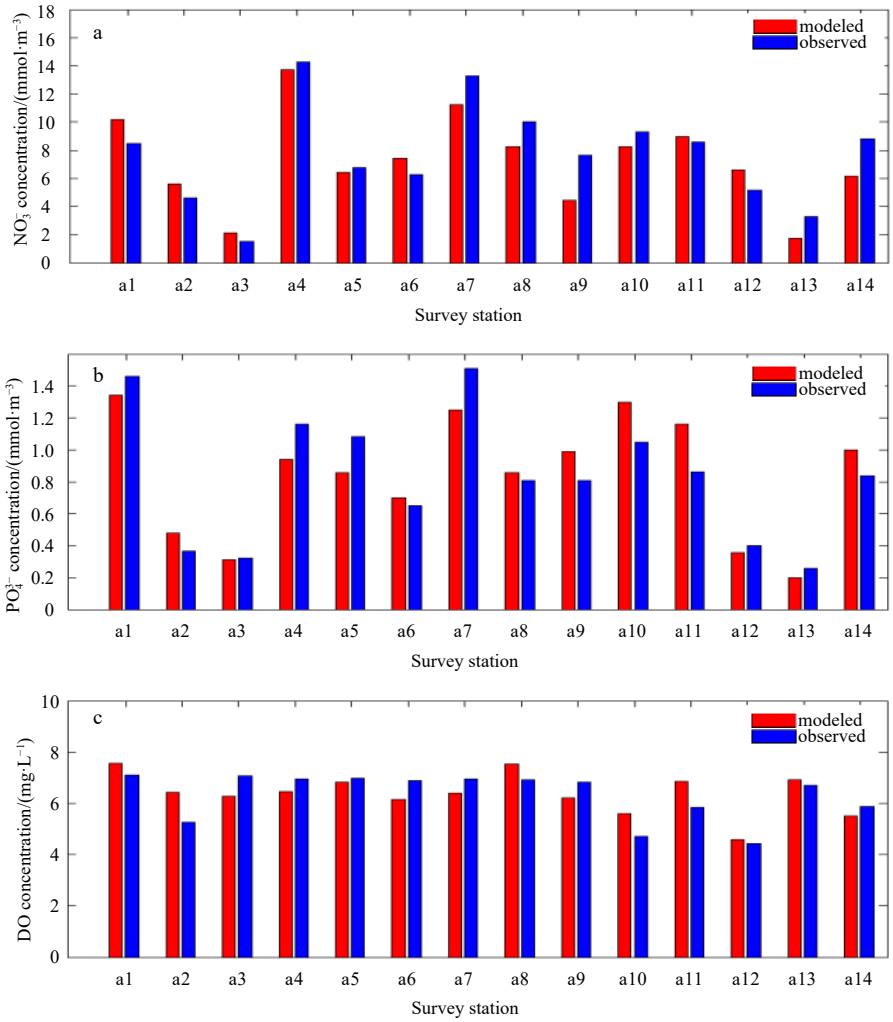

Fig. 5. The comparison between modeled results (red bars) and observed data (blue bars) of sea surface NO_3^- (a), PO_4^{3-} (b), and DO (c) at the stations in Fig. 1b in August 2011.

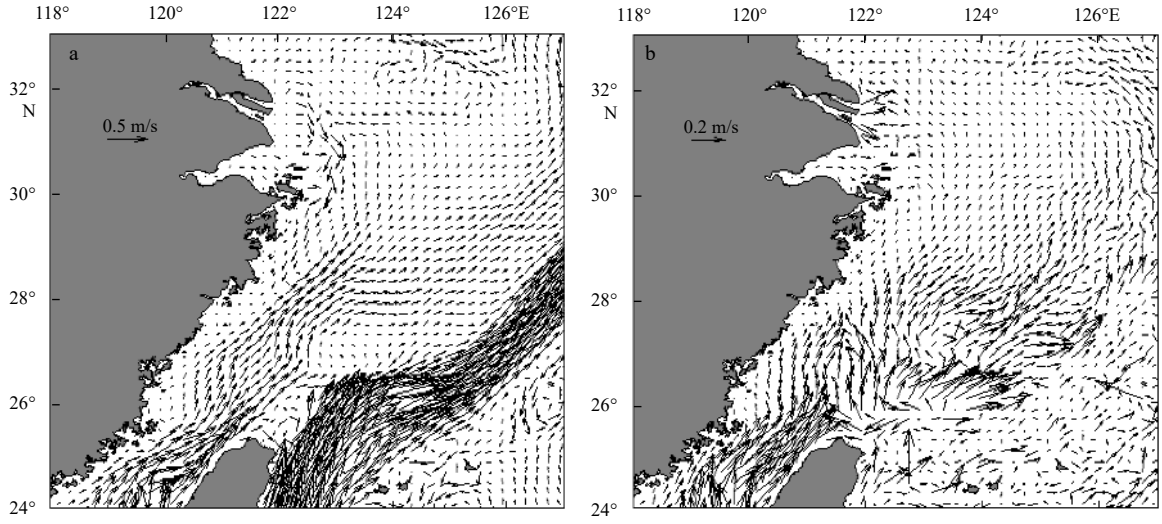

Fig. 6. Model monthly mean circulation at 10 m depth in September 2010 (a), model monthly mean circulation at sea bottom in September 2010 (b).

ginal N cycle, and the other settings were the identical. The time series of simulated hypoxic areas between the Base and N-only simulation were similar (Fig. 8). We quantified the hypoxic extent by calculating integrated hypoxic area that had the bottom

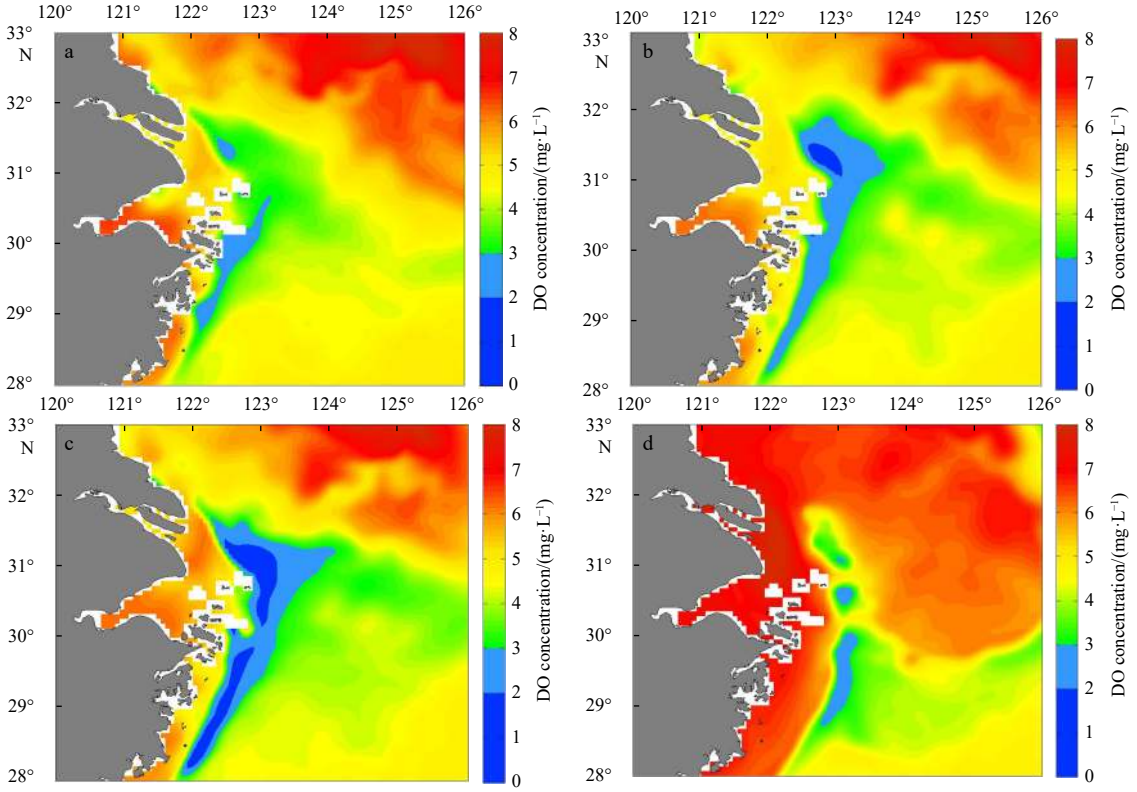

Fig. 7. The simulated results of the distribution of hypoxic zone off the Changjiang River Estuary in 2010 (a. July, b. August, c. September, d. October).

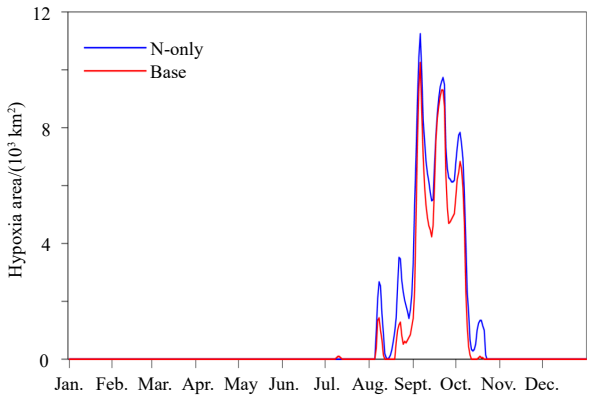

Fig. 8. The simulated hypoxic area (DO concentration<2 mg/L) between the Base and N-only simulations.

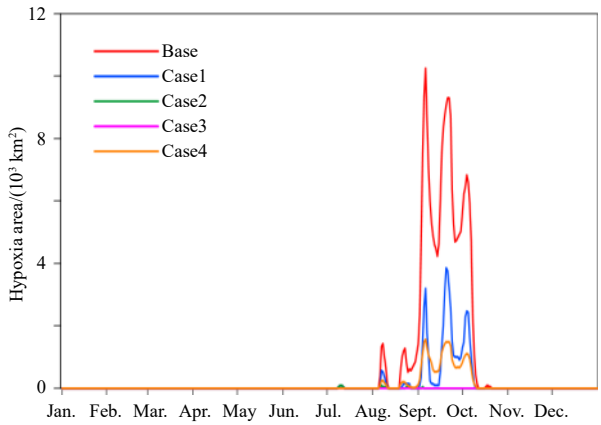

Fig. 9. The comparison of the simulated hypoxic area (DO concentration<2 mg/L) among the sensitivity experiments.

DO concentration below 2 mg/L at each day and integrated over all days in 2010. This comparison also reveals that, in the N-only run (simulation without P limitation), the integrated hypoxic area reached 330.5×10^3 km^2, while it was 250.1×10^3 km^2 in the Base run (simulation with P limitation), a decrease of the integrated hypoxic area by 24%.

3.4 *The contribution of different nutrient sources to the hypoxia off the Changjiang River Estuary*

The input from different nutrient sources strongly influenced the simulated hypoxic area. By calculating the total area of water with bottom DO concentration below the threshold value (<2 mg/L), the extent of the hypoxia can be quantified. In the Base run, the hypoxic zone developed from August to October, peaking in September (Fig. 9). Our results agreed with previous studies (Wei et al., 2015). In Case1, without the the nutrients input from the Taiwan Strait, the seasonal variation of the hypoxic area was almost equivalent to the Base run. The integrated hypoxic area and the Low DO was reduced by 77.8%, and 51.1%, respectively. In Case2, without the nutrients input from the Kuroshio, the hypoxic area was almost 0 km^2, which was consistent with Case3, and Low DO was decreased by 86.1%. In Case3, when there was no nutrients input from the Kuroshio and Taiwan Strait, the hypoxia disappeared, and the areas of Low DO were almost decreased to zero (Table 3). In Case4, without nutrients input from the Changjiang River, the hypoxic area off the Changjiang River Estuary was decreased sharply. The hypoxic area de-

Table 3. The total area of hypoxic area under different thresholds of DO concentration

Experiment	Integrated hypoxic area/(10^3 km^2)	
	<2 mg/L (hypoxia)	<3 mg/L (Low DO)
Base	250.1	1 021.6
Case1	55.4 (–77.8%)	499.2 (–51.1%)
Case2	0.7 (–99.7%)	142.1 (–86.1%)
Case3	0 (–100.0%)	3.3 (–99.7%)
Case4	37.0 (–85.2%)	274.5 (–73.1%)

Note: Low DO indicates dissolved oxygen concentration between 2 mg/L and 3 mg/L.

creased by 85.2% and Low DO decreased by 73.1% (Table 3). From the comparison of the these sensitivity experiments, we can conclude that the hypoxia off the Changjiang River Estuary was mainly affected by the nutrients input from the Kuroshio, followed by the Changjiang River, and the nutrients from the Taiwan Strait had the least contribution to the hypoxia.

3.5 *Changes in surface nutrients off the Changjiang Estuary*

In Case1, when the nutrient inputs from the Taiwan Strait were set to 0 mmol/m^3, the distribution of NO_3^- was consistent with the Base run, though the value of NO_3^- concentration was somewhat lower than Base run in the area of 30.5°–31.5°N, 123°–125°E (Fig. 10b). In Case2, when the nutrient inputs were from the Taiwan Strait and Changjiang River, the concentration of NO_3^- decreased rapidly eastward to the open shelf. The distribution of NO_3^- was mainly extended northward, with the high value area of NO_3^- concentration distributed north of 30.5°N. Compared with the Base run, the concentration of NO_3^- in the south of 30.5°N and the area of 30.5°–31.5°N, 123°–125°E was significantly decreased (Fig. 10c). In Case3, the NO_3^- originated only from the Changjiang River and it mainly extended northward in summer due to the southward monsoon (Chang and Isobe, 2003). In Case3, the NO_3^- distribution was mainly present at the north of 30.5°N, while it was negligible at the south of 30.5°N (Fig. 10d). The NO_3^- distribution in Case3 was similar with that of Case2. In order to quantitatively examine the nutrient influence from different origins on the hypoxia off the Changjiang River Estuary, two hypoxic zones (Box1, Box2) were selected (Fig. 1b). The model daily mean NO_3^- amount in Box1 and Box2 were carefully calculated from July to October 2010, respectively (Figs 10e, f).

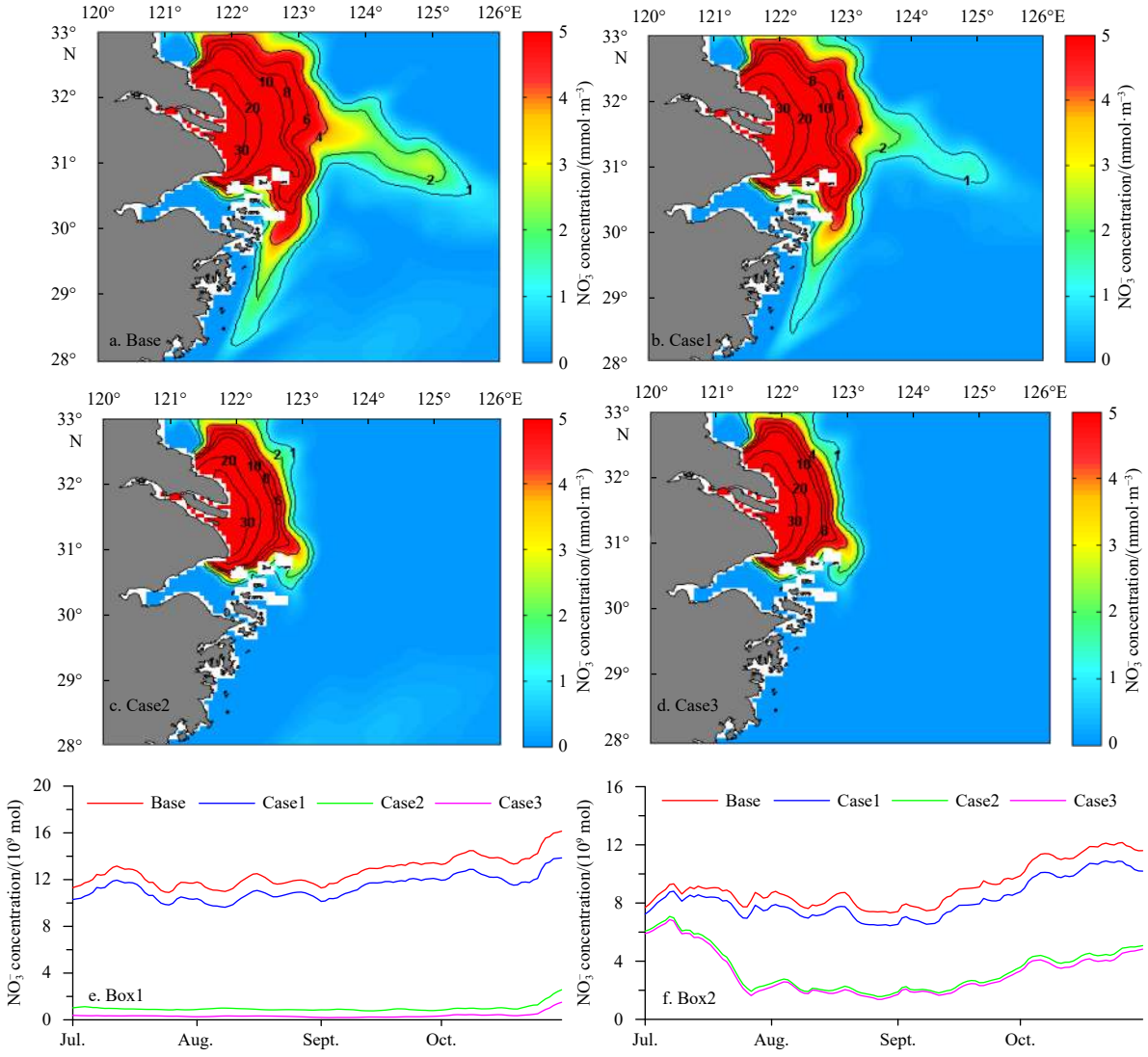

Fig. 10. The monthly mean NO_3^- concentration distribution at the sea surface in September 2010 among the different sensitivity experiments (a–d). The total NO_3^- amount in Box1 (e) and Box2 (f) (refer to Fig. 1b) from July to October, respectively.

The trend and value of NO_3^- concentration in Case1 were similar to the Base run, both in southern region (Box1) and northern region (Box2). Furthermore, the NO_3^- concentration in Case1 was nearly an order of magnitude larger than that of Case2 and Case3 in the Box1. This indicated that off the coast of Zhejiang, the NO_3^- was mainly sourced from the Kuroshio, and that the amount of nutrients transported from the Taiwan Strait or the Changjiang River was very small. A similar result was reported by Liu et al. (2000).

From the comparison of PO_4^{3-} distributions in Case1 and Case2 (Figs 11b, c), we determined that the PO_4^{3-} concentration was higher in Case1 off the coast of Zhejiang and the area of 31°–32°N, 121.5°–123°E, but lower in the area of 30°–31°N, 123°–126°E. While in Case3 PO_4^{3-} concentration was sharply reduced. The PO_4^{3-} concentrations in Case1 contributed to Box1 and Box2 more than in Case2 (Figs 11e, f). In Case3, the PO_4^{3-} concentration was the lowest compared with that of Case1 or Case2. Therefore, the PO_4^{3-} presents off the Changjiang River Estuary originated mainly from the Kuroshio, with less input from the Taiwan Strait and Changjiang River.

4 Discussion

The coupled physical-biological model for the ECS was applied to investigate the development of hypoxia off the Changjiang River Estuary in 2010. The spatial patterns of simulated nutrients, DO and Chl were similar to those collected from *in situ* observations and remotely sensed data. However, in some areas there were deviations from the observed results. These may have arisen from the use of monthly averaged data for the Changjiang River nutrient inputs, due to insufficient observed data. The results of model validation determined that the coupled model of ROMS-Fennel can successfully reproduce the variations of biological variables and the hypoxia off the Changjiang River Estuary.

4.1 *The effect of P limitation on the hypoxia off the Changjiang River Estuary*

The P limitation reduced the magnitude of hypoxia compared with the N-only simulation. We attribute this to the fact that P limitation dilutes the effect of eutrophication off the Changjiang River Estuary. As a result, it reduces the primary production, which will lead to less DO consumption by organic mat-

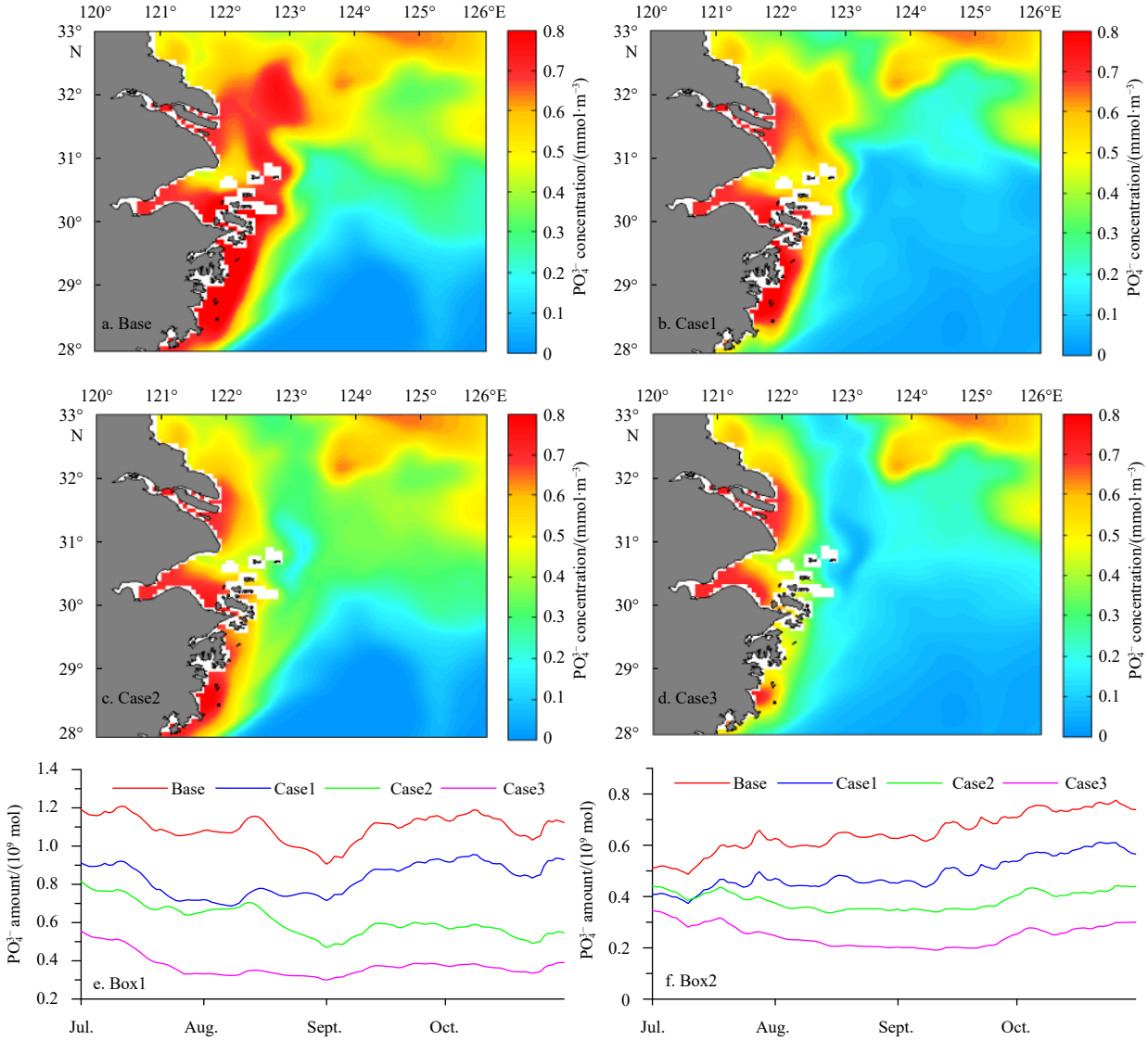

Fig. 11. The monthly mean PO_4^{3-} concentration distribution at the sea surface in September 2010 among the different sensitivity experiments (a–d); the total PO_4^{3-} amount in Box1 (e) and Box2 (f) from July to October, respectively.

ter decomposition. Thus, bottom DO depletion is reduced, and hypoxia decrease. In future studies, we will explore the individual contribution of different nutrient (NO_3^- or PO_4^{3-}) to hypoxia off the Changjiang River Estuary. Furthermore, we will attempt to solve the more practical problems of how far the individual nutrients (N or P) or combined nutrients load would have to be reduced to effectively relieve the hypoxia.

4.2 *The influence of different source of nutrients on the hypoxia*

Since the distributions of NO_3^- and PO_4^{3-} in Case1 were similar to the Base run (Figs 10 and 11), the corresponding distribution of Chl was also comparable with the Base run, though slightly less (Figs12a, b). In Case1, when set the nutrients input from the Taiwan Strait to zero, it had little influence on the surface Chl, only impacted the surface Chl in the southern region (Box1) and the area of 30.5°–31.5°N, 124.0°–125.5°E. In addition, there were three high Chl concentration cores in the Base run and Case1. One was in the southern region (Box1), second was in the northern region (Box2) and the third of particular interest was located at the area of 30.5°–31.5°N, 124.0°–125.5°E. In Case1, the total Chl amount was tightly correlated with the Base run both in Box1 and especially in Box2 (Figs 12e, f). Similarly, the volume-averaged Chl in September reduced by 11% in southern region and 4% in the northern region compared with Base run (Table 4). In Case2, removing the nutrients input from the Kuroshio had strongly effect on the surface Chl in the southern region (Box1). Surface Chl also decreased in the northern region, especially near Zhoushan Islands (Fig. 12c). The volume-averaged Chl in southern region and northern region decreased by 69% and 23% relative to the Base run , respectively (Table 4). In Case3, when there was no nutrients input from the open ocean, the surface Chl maintained a high value in the northern region.

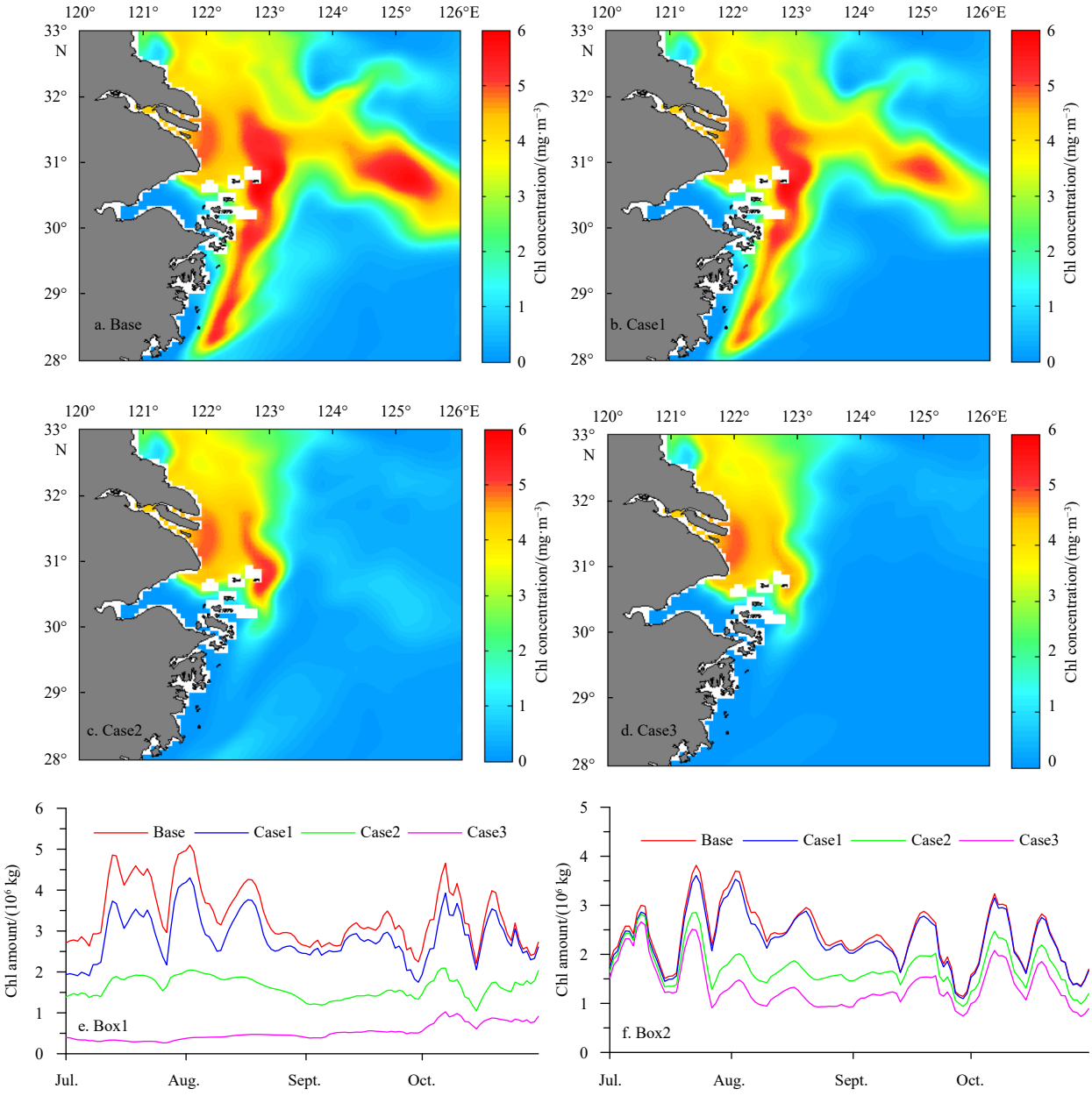

Fig. 12. The monthly mean chlorophyll (Chl) distribution at the sea surface in September 2010 among the sensitivity experiments (a–d). The total Chl amount in Box1 (e) and Box2 (f) from July to October, respectively.

Table 4. The volume-averaged chlorophyll concentration (mg/L) in sensitivity experiments in September 2010

Region	Base	Case1	Case2	Case3	Case4
Box1 (southern region)	1.54(100%)	1.37(89%)	0.48(31%)	0.18(12%)	1.36(88%)
Box2 (northern region)	3.24(100%)	3.12(96%)	2.48(77%)	2.20(68%)	1.89(58%)

While the monthly mean Chl deceased dramatically in the southern region and near the Zhoushan Islands. And we did not detect any high Chl concentration cores in the southern region, which is similar to Case2 (Figs 12c, d). Without the nutrients input from the Kuroshio and Taiwan Strait, the volume-averaged Chl in September reduced by 88% in southern region and 32% in the northern region.

In Case4, without the nutrients input from the Changjiang River had little effect on the surface Chl in the southern region. The high Chl concentration cores were still remained in the southern region and the area of 30.5°–31.5°N, 124.0°–125.5°E. However, the monthly mean surface Chl concentration was obviously decreased in the northern region (Fig. 13a). Removing the nutrients input from the Changjiang River, the volume-averaged Chl in southern region and northern region decreased by 12% and 42% compared with the Base run, respectively. In other words, the nutrients input from the Changjiang River fuel about 42% of Chl biomass in the northern region. Among the sensitivity experiments, the nutrients input from the Changjiang River made the largest contribution to Chl in the northern region. In a word, we can conclude that the Chl in the northern region (Box2) was mainly driven by the supply of nutrients from the Changjiang River. This was related to that the nutrients input from the Changjiang River extend northeastward in summer due to the prevailing southwest wind (Chang and Isobe, 2003). However, the Chl in the southern region (Box1) was controlled by the nutrients from the Kuroshio. The possible reason for this was that compared with the Changjiang River, the Kuroshio current provided a larger amount of nutrient to the ECS shelf to promote the growth of phytoplankton (Xu et al., 2018). And the nutrient input from the Taiwan Strait made little contribution to the Chl in the northern region and southern region. These results were consistent with the results reported in the study conducted by Xu et al. (2020).

In Case1, from the monthly mean DO concentration distribution at the bottom in September (Fig. 14b), the hypoxia disappeared, while the Low DO remained (Figs 14e, f). In Case1, the minimum value of DO concentration less than 2 mg/L appeared off the Changjiang River Estuary in August, September and early October which was the same as that in Base run. Additionally, in Case1, the minimum value of bottom DO concentration in Box1 and Box2 were reduced to 0.83 mg/L and 1.47 mg/L, respectively. Table 5 showed that without the nutrients input from the Taiwan Strait, the integrated Low DO area decreased by 45% in the southern region and 52% in the northern region with respect to the Base run. Among the four sensitivity experiments, the nutrients input from the Taiwan Strait has the least contribution to the integrated Low DO area. While in Case3, the hypoxia and Low DO both completely disappeared, and the minimum value of bottom of DO concentration was basically greater than 3 mg/L (Figs 14e, f). This was mainly due to a significant decrease in the Chl concentration, which lead to a decreased consumption of DO by the decomposition of organic matter, eventually resulting in an increased DO concentratrion in the bottom layer and the disappearance of hypoxia.

In Case2, due to a lack of NO_3^- in the south of 30.5°N, the Chl concentration was lower in this area than in the Base run. The hypoxia completely disappeared, and the zone of Low DO was almost negligible (Fig. 14c). The decrease in Chl concentration resulted in decreased DO consumption by the decaying of dead phytoplankton, which eventually lead to the disappearance of hypoxia. In Case2, there was no hypoxia off the Changjiang River Estuary from July to October (Figs 14e, f). The minimum value of bottom DO concentration in Box1 and Box2 were reduced to 2.11 mg/L and 2.21 mg/L, respectively, which was almost twice as much as Case1. Removing the nutrients input from the Kuroshio reduced the integrated Low DO area by 90% and 84% in the southern region and northern region, respectively (Table 5). This indicated that the hypoxia was dramatically influenced by the nutrient from the Kuroshio, and the contribution of Kuroshio nutrient to the Low DO in the southern region is slightly greater than that in the northern region.

In Case3, the concentration of Chl was the lowest among the sensitivity experiments (Fig. 12d). As a result, the bottom DO concentration was significantly increased and hypoxia was absent due to the decomposition of organic matter being reduced in the bottom water (Fig. 14d). The minimum value of DO concentration was generally greater than 4 mg/L in Box1, and greater than 3 mg/L in Box2 (Figs 14e, f). And the integrated Low DO area was almost reduced to zero both in the southern and north-

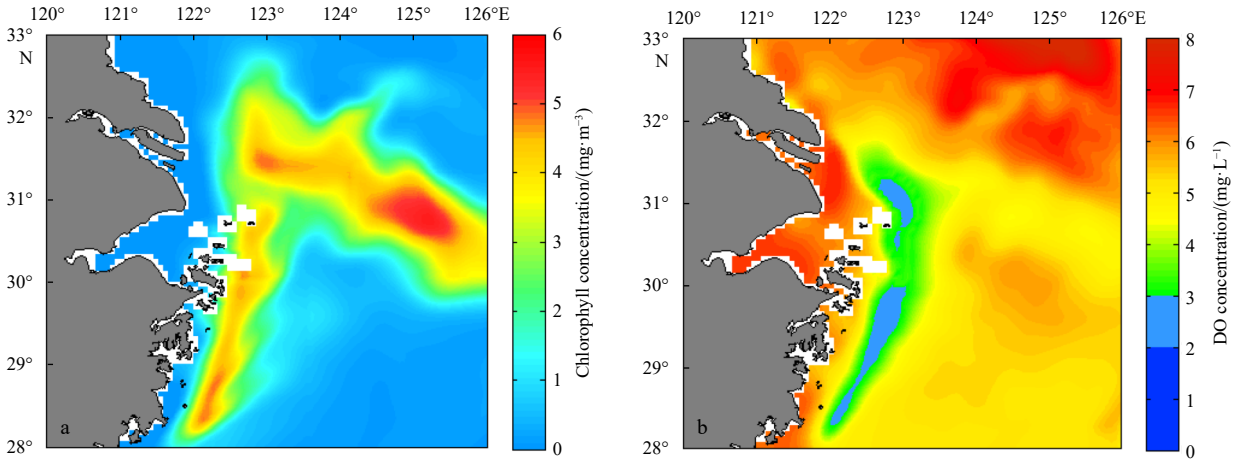

Fig. 13. The monthly mean chlorophyll concentration distribution at the sea surface in September 2010 in Case4 (a); the monthly mean DO concentration distribution at the sea bottom in September 2010 in Case4 (b).

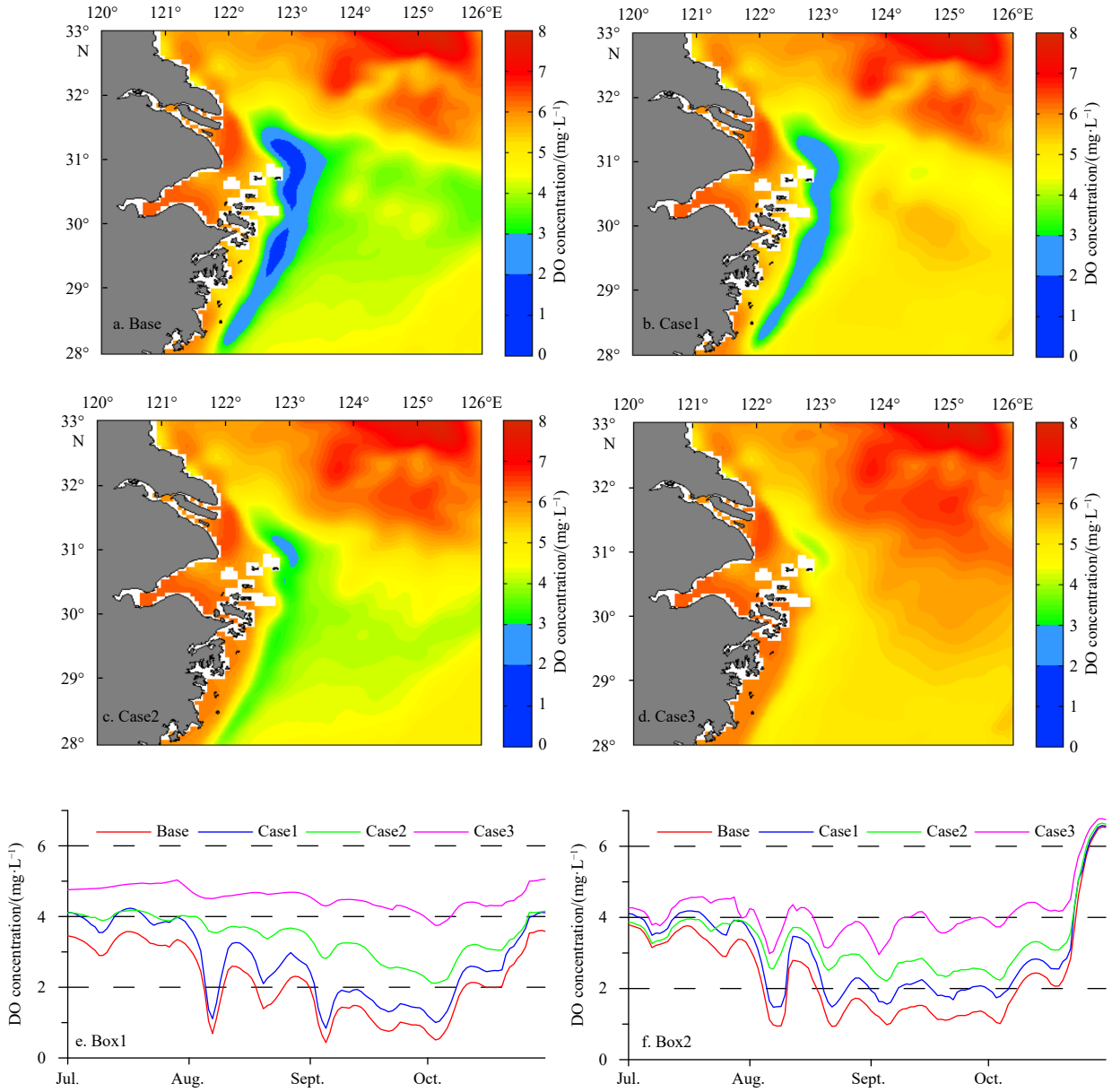

Fig. 14. The monthly mean DO concentration distribution at the bottom in September 2010 among the sensitivity experiments (a–d). The minimum value of DO concentration at the sea bottom water in Box1 (e) and Box2 (f) from July to October, respectively.

Table 5. Integrated Low DO area (10^3 km^2) in Box1 and Box2 in each experiment in 2010

	Base	Case1	Case2	Case3	Case4
Box1 (southern region)	415(100%)	227(55%)	41(10%)	0(0%)	178(43%)
Box2 (northern region)	555(100%)	264(48%)	90(16%)	2(0%)	90(16%)

Note: Low DO indicates dissolved oxygen concentration between 2 mg/L and 3 mg/L.

ern regions (Table 5).

In Case4, when there was no nutrients input from the Changjiang River, the volume-averaged Chl decreased by 42% in northern region, which caused an increase in oxygen levels at the bottom layer through less decomposition of organic matters. As a result, the DO concentration in bottom layer increased significantly (Fig. 13b), and the integrated Low DO area decreased by 84% in the northern region (Table 5). In the southern region, the volume-averaged Chl was obviously greater than that in the northern region, which would lead to more DO consumption. Thus, the integrated Low DO area in the southern region was remarkably larger than that in the northern region. In other words, the nutrients input from the Changjiang River made more contribution to hypoxia in the northern region than that in the southern region.

Above all, it can be concluded that the nutrients input from the Kuroshio contributed most to the hypoxia off the Changjiang River Estuary. The nutrients input from the Changjiang River played a more important role in the hypoxia in the northern region than that in the southern region. And the hypoxia off the Changjiang River Estuary was not strongly affected by the nutrients input from the Taiwan Strait. Zhou et al. (2017) illustrated that what are the roles of nutrient from the river and Kuroshio in the hypoxia off the Changjiang River Estuary. The author found that the maximum hypoxia extent increased by 29% associated

with the Kuroshio nutrient up 25%, while the maximum hypoxia extent increased by 14% with the riverine nutrient up 30%. This showed that the Kuroshio nutrient had a greater effect on the hypoxia off the Changjiang River Estuary with respect to the riverine nutrient. These findings are consistent with our results.

4.3 *Mechanisms of nutrient transport and influence on hypoxia*

Off the coast of Zhejiang, the high nutrient and Chl concentrations were reproduced in the numerical experiment of Case1. We propose a forcing mechanism to explicate this phenomenon (Fig. 15). During the process of the Kuroshio mainstream turning from the east of Taiwan Island to the northeast, the northwestern Kuroshio subsurface water is detached from the Kuroshio mainstream, forming a nearshore Kuroshio branch current (NKBC) (yellow arrows, Fig. 15). The NKBC continuously transported the nutrients from the Kuroshio to the bottom water off the coast of Zhejiang, bringing them to the surface through the upwelling. The upwelling off the coast of Zhejiang was influenced by the combination of CDW and TWC. The TWC flowed almost parallel to the coast of China in the upper 60 m depth until it reached 28°N (blue arrows, Fig. 15), before suddenly turning east. Due to the large velocity shear effect of the southward CDW and the northeastward TWC, it had strong positive vorticity that caused a strong upwelling off the coast of Zhejiang. Therefore, the bottom PO_4^{3-} and NO_3^- were absorbed by the phytoplankton through the upwelling to euphotic layer, which promoted the growth of phytoplankton, and increased the concentration of Chl off the coast of Zhejiang. In addition, the NO_3^- and PO_4^{3-} carried by the upwelling off the coast of Zhejiang were further transported to the areas of 30.5°–31.5°N, 124.0°–125.5°E by the northeastward TWC. In this area, a large density of phytoplankton with a constant supply of NO_3^- and PO_4^{3-}, resulted in a high Chl concentration. Due to the high concentration of Chl off the coast of Zhejiang, the bottom DO concentration was reduced through continued decomposition of organic matter, ultimately leading to hypoxia off the coast of Zhejiang. We propose that the hypoxia off the coast of Zhejiang was likely attributed to the NKBC and upwelling.

5 Conclusions

In this study, we utilized a physical-biogeochemical model to investigate the influence of various nutrient sources on the hypoxia off the Changjiang River Estuary. Our model was comparable with observations and reasonably reproduced the variability of biological variables and the distribution of hypoxia. We illustrated the effect of P limitation inducing a reduction in hypoxia off the Changjiang River Estuary. Simulations also demonstrated that the different sources of nutrients had various impacts on the bottom DO concentrations and hypoxia formation off the Changjiang River Estuary. When the nutrients originated from the Changjiang River and Kuroshio, the distribution of nutrients off the coast of Zhejiang showed good consistency with the Base run, and also maintained high Chl content. Ultimately, although the hypoxic area was decreased, the seasonal variation in the hypoxic area was almost coincident with the Base run. The nutrients input from the Taiwan Strait had little impact on the hypoxia in the northern region and southern region. Adjusting the nutrients inputs from the Kuroshio to zero led to the significantly reduction in the concentrations of nutrients and Chl off the coast of Zhejiang, which resulted in the disappearance of hypoxia, and Low DO decreased by 86.1%. When there were no nutrients input from the open ocean, both nutrients and Chl were further reduced, resulting in the disappearance of the hypoxia and Low DO conditions. Without the nutrients input from the Changjiang River, the integrated Low DO decreased by 84% in the northern region and 57% in the southern region, respectively. The nutri-

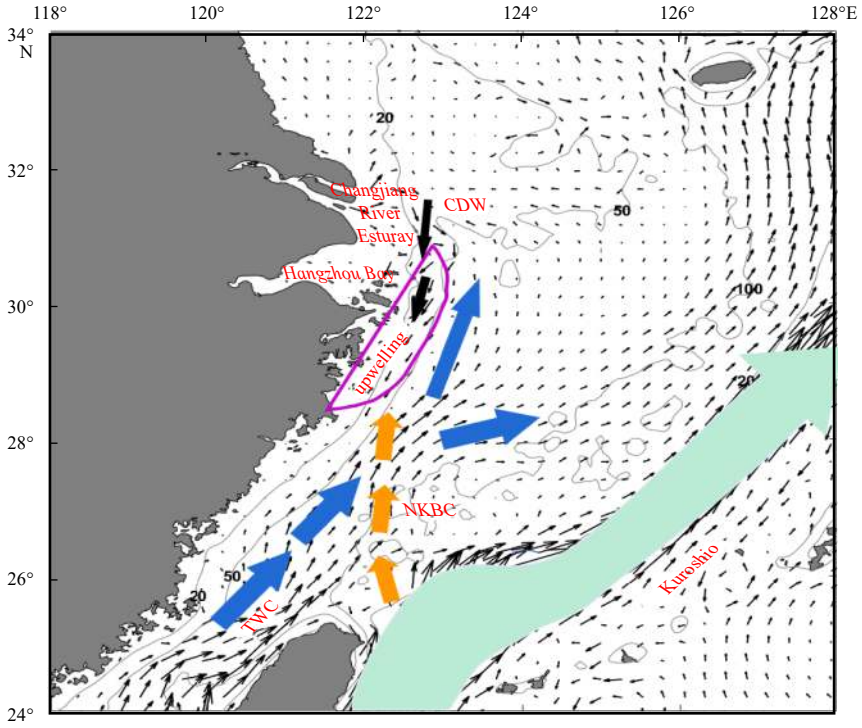

Fig. 15. The main ocean current pattern in the East China Sea in summer 2010 where the isobaths of 20 m, 50 m, 100 m, 200 m are overlapped. The blue arrows represent the Taiwan Warm Current (TWC); the yellow arrows represent the nearshore Kuroshio branch current (NKBC); and the black arrows represent the Changjiang diluted water (CDW). The upwelling is indicated by the pink cycle.

ents input from the Changjiang River contributed more to the hypoxia in the northern region than that in the southern region.

Overall, the nutrients input from the Kuroshio make the most contribution to the development of hypoxia off the Changjiang River Estuary, follow by the Changjiang River, and The Taiwan Strait have the smallest contribution. Although the hypoxia off the Changjiang River Estuary is more responsive to the Kuroshio nutrient than the riverine nutrient, the nutrients input from the Changjiang River have a direct effect on the hypoxia. This implies that reducing the riverine nutrients loading is likely to reduce the hypoxia, effectively.

References

Boesch D F, Rabalais N N. 1991. Effects of hypoxia on continental shelf benthos: comparisons between the New York Bight and the Northern Gulf of Mexico. Geological Society, London, Special Publications, 58(1): 27–34, doi: 10.1144/gsl.sp.1991.058.01.02

Carnes M R. 2009. Description and Evaluation of GDEM-V 3.0. Washington: Naval Research Laboratory, Stennis Space Center

Chang P H, Isobe A. 2003. A numerical study on the Changjiang diluted water in the Yellow and East China Seas. Journal of Geophysical Research: Oceans, 108(C9): 3299, doi: 10.1029/2002JC001749

Chen Chen-Tung Arthur. 1996. The Kuroshio intermediate water is the major source of nutrients on the East China Sea continental shelf. Oceanologica Acta, 19(5): 523–527

Chen Yuh-Ling Lee, Chen Houng-Yung, Gong Gwo-Ching, et al. 2004. Phytoplankton production during a summer coastal upwelling in the East China Sea. Continental Shelf Research, 24(12): 1321–1338, doi: 10.1016/j.csr.2004.04.002

Chen Chung-Chi, Chiang Kuo-Ping, Gong Gwo-Ching, et al. 2006. Importance of planktonic community respiration on the carbon balance of the East China Sea in summer. Global Biogeochemical Cycles, 20: GB4001, doi: 10.1029/2005GB002647

Chen ChungChi, Gong GwoChing, Shiah F K. 2007. Hypoxia in the East China Sea: one of the largest coastal low-oxygen areas in the world. Marine Environmental Research, 64(4): 399–408, doi: 10.1016/j.marenvres.2007.01.007

Chen Yaxin, Liu Ruimin, Sun Chengchun, et al. 2012. Spatial and temporal variations in nitrogen and phosphorous nutrients in the Yangtze River Estuary. Marine Pollution Bulletin, 64(10): 2083–2089, doi: 10.1016/j.marpolbul.2012.07.020

Chen Jianyu, Pan Delu, Liu Mingliang, et al. 2017. Relationships between long-term trend of satellite-derived chlorophyll-*a* and hypoxia off the Changjiang Estuary. Estuaries and Coasts, 40(4): 1055–1065, doi: 10.1007/s12237-016-0203-0

Chen Chen-Tung Arthur, Wang Shulun, 1999. Carbon, alkalinity and nutrient budgets on the East China Sea continental shelf. Journal of Geophysical Research: Oceans, 104(C9): 20675–20686, doi: 10.1029/1999jc900055

Diaz R J, Rosenberg R. 1995. Marine benthic hypoxia: a review of its ecological effects and the behavioural responses of benthic macrofauna. Oceanography and Marine Biology, 33: 245–303

Diaz R J, Rosenberg R. 2008. Spreading dead zones and consequences for marine ecosystems. Science, 321(5891): 926–929, doi: 10.1126/science.1156401

Egbert G D, Erofeeva S Y. 2002. Efficient inverse modeling of barotropic ocean tides. Journal of Atmospheric and Oceanic Technology, 19(2): 183–204, doi: 10.1175/1520-0426(2002)019<0183:EIMOBO>2.0.CO;2

Fang Tien-Hsi. 2004. Phosphorus speciation and budget of the East China Sea. Continental Shelf Research, 24(12): 1285–1299, doi: 10.1016/j.csr.2004.04.003

Fennel K, Hu Jiatang, Laurent A, et al. 2013. Sensitivity of hypoxia predictions for the northern Gulf of Mexico to sediment oxygen consumption and model nesting. Journal of Geophysical Research: Oceans, 118(2): 990–1002, doi: 10.1002/jgrc.20077

Fennel K, Wilkin J, Levin J, et al. 2006. Nitrogen cycling in the Middle Atlantic Bight: results from a three-dimensional model and implications for the North Atlantic nitrogen budget. Global Biogeochemical Cycles, 20(3): GB3007, doi: 10.1029/2005GB002456

Gao Lei, Li Daoji, Zhang Yanwei. 2012. Nutrients and particulate organic matter discharged by the Changjiang (Yangtze River): seasonal variations and temporal trends. Journal of Geophysical Research: Biogeosciences, 117(G4): G04001, doi: 10.1029/2012JG001952

Gong Gwo-Ching, Chen Yuh-Ling Lee, Liu Kon-Kee. 1996. Chemical hydrography and chlorophyll *a* distribution in the East China Sea in summer: implications in nutrient dynamics. Continental Shelf Research, 16(12): 1561–1590, doi: 10.1016/0278-4343(96)00005-2

Große F, Fennel K, Zhang Haiyan, et al. 2020. Quantifying the contributions of riverine vs. oceanic nitrogen to hypoxia in the East China Sea. Biogeosciences, 17(10): 2701–2714, doi: 10.5194/bg-17-2701-2020

Hu Jianyu, Kawamura H, Li Chunyan, et al. 2010. Review on current and seawater volume transport through the Taiwan Strait. Journal of Oceanography, 66(5): 591–610, doi: 10.1007/s10872-010-0049-1

Isobe A. 2008. Recent advances in ocean-circulation research on the Yellow Sea and East China Sea shelves. Journal of Oceanography, 64(4): 569–584, doi: 10.1007/s10872-008-0048-7

Karlson K, Rosenberg R, Bonsdorff E. 2002. Temporal and spatial large-scale effects of eutrophication and oxygen deficiency on benthic fauna in Scandinavian and Baltic waters—a review. Oceanography and Marine Biology: An Annual Review, 40: 427–489

Li Hongliang, Chen Jianfang, Lu Yunke, et al. 2011. Seasonal variation of DO and formation mechanism of bottom water hypoxia of Changjiang River Estuary. Journal of Marine Sciences, 29(3): 78–87

Li Hongmei, Shi Xiaoyong, Wang Hao, et al. 2014. An estimation of nutrient fluxes to the East China Sea continental shelf from the Taiwan Strait and Kuroshio subsurface waters in summer. Acta Oceanologica Sinica, 33(11): 1–10, doi: 10.1007/s13131-014-0550-2

Liu Xincheng, Shen Huanting, Huang Qinghui. 2002. Concentration variation and flux estimation of dissolved inorganic nutrient from the Changjiang River into its estuary. Oceanologia et Limnologia Sinica, 33(3): 332–340

Liu Kon-Kee, Tang TswenYung, Gong Gwo-Ching, et al. 2000. Cross-shelf and along-shelf nutrient fluxes derived from flow fields and chemical hydrography observed in the southern East China Sea off Northern Taiwan. Continental Shelf Research, 20(4–5): 493–523, doi: 10.1016/S0278-4343(99)00083-7

Liu Kon-Kee, Yan Weijin, Lee Hung-Jen, et al. 2015. Impacts of increasing dissolved inorganic nitrogen discharged from Changjiang on primary production and seafloor oxygen demand in the East China Sea from 1970 to 2002. Journal of Marine Systems, 141: 200–217, doi: 10.1016/j.jmarsys.2014.07.022

Lu Wenhai, Xiang Xianquan, Yang Lu, et al. 2017. The temporal-spatial distribution and changes of dissolved oxygen in the Changjiang Estuary and its adjacent waters for the last 50 a. Acta Oceanologica Sinica, 36(5): 90–98, doi: 10.1007/s13131-017-1063-6

Morel A, Berthon J F. 1989. Surface pigments, algal biomass profiles, and potential production of the euphotic layer: relationships reinvestigated in view of remote-sensing applications. Limnology and Oceanography, 34(8): 1545–1562, doi: 10.4319/lo.1989.34.8.1545

Ning Xiuren, Lin Chuanlan, Su Jilan, et al. 2011. Long-term changes of dissolved oxygen, hypoxia, and the responses of the ecosystems in the East China Sea from 1975 to 1995. Journal of Oceanography, 67(1): 59–75, doi: 10.1007/s10872-011-0006-7

Rabalais N N, Díaz R J, Levin L A, et al. 2010. Dynamics and distribution of natural and human-caused hypoxia. Biogeosciences, 7(2): 585–619, doi: 10.5194/bg-7-585-2010

Renaud M L. 1986. Hypoxia in Louisiana coastal waters during 1983:

implications for fisheries. Fishery Bulletin, 84(1): 19–26
Wang Baodong. 2009. Hydromorphological mechanisms leading to hypoxia off the Changjiang Estuary. Marine Environmental Research, 67(1): 53–58, doi: 10.1016/j.marenvres.2008.11.001
Wang Kui, Cai Weijun, Chen Jianfang, et al. 2021. Climate and human-driven variability of summer hypoxia on a large river-dominated shelf as revealed by a hypoxia index. Frontiers in Marine Science, 8: 634184, doi: 10.3389/fmars.2021.634184
Wang Wentao, Cao Xihua, Yuan Yongquan, et al. 2016. Variation and controlling factor of nutrient distribution in Changjiang River Estuary and adjacent areas in 2012. Oceanologia et Limnologia Sinica, 47(4): 804–812, doi: 10.11693/hyhz20160100017
Wang Baodong, Wei Qinsheng, Chen Jianfang, et al. 2012. Annual cycle of hypoxia off the Changjiang (Yangtze River) Estuary. Marine Environmental Research, 77: 1–5, doi: 10.1016/j.marenvres.2011.12.007
Wang Jianing, Yan Weijin, Chen Nengwang, et al. 2015. Modeled long-term changes of DIN: DIP ratio in the Changjiang River in relation to Chl-α and DO concentrations in adjacent estuary. Estuarine, Coastal and Shelf Science, 166: 153–160, doi: 10.1016/j.ecss.2014.11.028
Wei Hao, He Yunchang, Li Qingji, et al. 2007. Summer hypoxia adjacent to the Changjiang Estuary. Journal of Marine Systems, 67(3–4): 292–303, doi: 10.1016/j.jmarsys.2006.04.014
Wei Qinsheng, Wang Baodong, Chen Jianfang, et al. 2015. Recognition on the forming-vanishing process and underlying mechanisms of the hypoxia off the Yangtze River estuary. Science China: Earth Sciences, 58(4): 628–648, doi: 10.1007/s11430-014-5007-0
Xu Lingjing, Yang Dezhou, Benthuysen J A, et al. 2018. Key dynamical factors driving the Kuroshio subsurface water to reach the Zhejiang coastal area. Journal of Geophysical Research: Oceans, 123(12): 9061–9081, doi: 10.1029/2018JC014219
Xu Lingjing, Yang Dezhou, Greenwood J, et al. 2020. Riverine and oceanic nutrients govern different algal bloom domain near the Changjiang Estuary in summer. Journal of Geophysical Research: Biogeosciences, 125(10): e2020JG005727, doi: 10.1029/2020JG005727
Zhang Haiyan, Fennel K, Laurent A, et al. 2020. A numerical model study of the main factors contributing to hypoxia and its inter-annual and short-term variability in the East China Sea. Biogeosciences, 17(22): 5745–5761, doi: 10.5194/bg-17-5745-2020
Zhang Jing, Liu Sumei, Ren Jingling et al. 2007. Nutrient gradients from the eutrophic Changjiang (Yangtze River) Estuary to the oligotrophic Kuroshio waters and re-evaluation of budgets for the East China Sea shelf. Progress in Oceanography, 74(4): 449–478, doi: 10.1016/j.pocean.2007.04.019
Zheng Jingjing, Gao Shan, Liu Guimei, et al. 2016. Modeling the impact of river discharge and wind on the hypoxia off Yangtze Estuary. Natural Hazards and Earth System Sciences, 16(12): 1–25, doi: 10.5194/nhess-2016-129
Zhou Feng, Chai Fei, Huang Daji, et al. 2017. Investigation of hypoxia off the Changjiang Estuary using a coupled model of ROMS-CoSiNE. Progress in Oceanography, 159: 237–254, doi: 10.1016/j.pocean.2017.10.008
Zhou Feng, Chai Fei, Huang Daji, et al. 2020. Coupling and decoupling of high biomass phytoplankton production and hypoxia in a highly dynamic coastal system: the Changjiang (Yangtze River) Estuary. Frontiers in Marine Science, 7: 259, doi: 10.3389/fmars.2020.00259
Zhou Feng, Huang Daji, Ni Xiaobo, et al. 2010. Hydrographic analysis on the multi-time scale variability of hypoxia adjacent to the Changjiang River Estuary. Acta Ecologica Sinica, 30(17): 4728–4740
Zhu Zhuoyi, Zhang Jing, Wu Ying, et al. 2011. Hypoxia off the Changjiang (Yangtze River) Estuary: oxygen depletion and organic matter decomposition. Marine Chemistry, 125(1–4): 108–116, doi: 10.1016/j.marchem.2011.03.005